ELSEVIER

PII: S0032-3861(97)10276-2

Polymer Vol. 39 No. 22, pp. 5483–5493, 1998

0032-3861/98/$ - see front matter

Preparation, structure, growth mechanisms and properties of siloxane composites containing silica, titania or mixed silica–titania phases

J. M. Breiner and J. E. Mark*
Department of Chemistry and the Polymer Research Center, The University of Cincinnati, Cincinnati, OH 45221-0172, USA
(Received 18 July 1997; accepted 7 November 1997)

Poly(dimethylsiloxane) (PDMS) [–Si$(CH_3)_2$O–] networks were prepared by tetrafunctionally endlinking hydroxyl-terminated chains with tetraethoxysilane. Composites were prepared by *in situ* base-catalysed hydrolysis of an organosilicate and an organotitanate, resulting in the formation of reinforcing silica, titania or silica–titania mixed-oxide fillers within the networks. The growth processes and resulting structures of the reinforcing fillers were studied by small-angle X-ray scattering. Both systems were found to yield dense particles with fractally rough surfaces. Some of the scattering results were used to interpret previously reported mechanical properties obtained on such composites using equilibrium stress–strain measurements in elongation. Of particular interest were mixed silica–titania fillers, since in at least some cases these are known to reinforce PDMS networks better than either silica or titania alone. The scattering results suggest that the corresponding growth processes proceed by the formation of relatively uniform titania particles, followed by the formation of significantly larger silica particles.

(Keywords: poly(dimethylsiloxane); reinforcement; silica)

INTRODUCTION

The production of *in situ* reinforced polymeric composites by sol–gel processes is developing rapidly, but there is still a need for a better molecular understanding of their syntheses, structures and properties[1–6]. In this application, the sol–gel process is quite complicated, consisting of the hydrolysis and condensation of appropriate alkoxy compounds within an organic polymer matrix, to create reinforcing inorganic ceramic phases. Examples are the hydrolysis of a silicate to silica, a titanate to titania, and a zirconate to zirconia.

One polymer that has been much used in such investigations is poly(dimethylsiloxane) (PDMS) [–Si$(CH_3)_2$O–]. It is a semi-inorganic polymer with high thermal stability, low glass transition temperature, good weather resistance, low surface tension, and unusually high permeability[7–9]. One major shortcoming is that elastomers prepared from PDMS are relatively weak materials in the unfilled state. Therefore they generally require a reinforcing filler in most of their applications in order to take full advantage of the attractive properties cited. The usual industrial processing of these materials involves an energy-intensive *ex situ* blending of a reinforcing filler, most commonly fumed silica, into the PDMS prior to its crosslinking. Processing problems with this technique have encouraged the alternative of incorporating the silica through sol–gel *in situ* precipitations. This newer approach permits good control of particle sizes and size distributions, while avoiding agglomeration of the reinforcing particles.

Until recently, a detailed understanding of the interactions of a highly dispersed inorganic filler within an organic polymer was limited by methods for characterizing the microstructure of these materials. There has also been a lack of reasonable models capable of predicting their growth and structure based solely on chemical and physical parameters. However, with advances in instrumentation and the development of concepts to model growth processes in complex disordered systems, the solutions to some of these problems can now be achieved[10–13].

The primary goal of the present research project was to develop a better understanding of the structure/property relationships in some of these high-performance materials. Silica, titania and silica–titania mixed oxides were chosen as the inorganic phases, and PDMS as the elastomeric host matrix. The first part of the project employed the now-standard synthetic pathways developed for the *in situ* reinforcement of PDMS[1–6, 14–16]. The second part examined the structure of the titania phase and of the co-silica–titania phase as a function of the synthetic pathways employed. By employing small-angle X-ray scattering (SAXS) and the concepts of fractal geometry, a series of experiments was developed to derive the structures of the inorganic phase of the composites. These measurements were carried out in the solid state, in contrast to the work of Schaefer and Keefer[13] who conducted some related scattering experiments in solutions. The third part employed the scattering results to interpret some previously reported mechanical properties[6,15] obtained for such composites from equilibrium stress–strain measurements in elongation.

RELEVANT BACKGROUND INFORMATION

Fractal concepts

Fractals are disordered systems whose disorder can be described in terms of non-integral or fractional dimensions[17]. Relevant here is the opportunity to characterize the

* To whom correspondence should be addressed

interplay between shape and structure and the processes which form these structures, or the processes which take place in the environments created by these structures[18].

Fractal structures can be characterized by a single parameter D, the fractal dimension, which is defined as the exponent that relates an object's mass M to its size R[17–19]:

$$M \propto R^D \tag{1}$$

There are a variety of kinetic growth models that give rise to disordered structures with various fractal dimensions. If the mass and surface scale alike, the system is called a mass fractal and the structure can be described by equation (1). Mass fractals resemble polymeric-like structures. The mass fractal dimension D can assume any value in the range $1 < D < 3$. At the lower limit as D approaches 1, a linear object is expected, and at $D = 3$, the object is uniformly dense. Intermediate values represent more complex structures. For example, if $D = 5/3$, the disordered system must occupy intrinsically more space than a linear chain or a planar surface[18].

Surface fractals are uniformly dense, colloidal-like structures with a fractally rough surface. They are characterized by a surface fractal dimension D_s which relates the surface area S of an object to its radius a:

$$S = a^{D_s} \tag{2}$$

The corresponding fractal dimensions can assume any value in the range $2 < D_s < 3$. When $D_s = 2$, the surface of an object is uniformly smooth, such as that of a marble. A surface fractal dimension of 3 corresponds to a rough surface, such as the land surface of the earth.

Some examples of models representing mass fractals are the Witten–Sander and Sutherland models, and some representing surface fractals are the Eden and Vold models[20–22].

Scattering from fractals

Small-angle scattering is one of the most useful experimental techniques for determining fractal dimensions. Fractal objects lack the rotational and translational symmetry of regular objects, but they do possess a form of symmetry called dilational. In this type of symmetry, the general shape of the structure does not change with a transformation of scale[23]. That is, it remains self-similar.

Mathematically, self-similarity requires a power-law relationship between the structural parameters such as size and mass. Because of this, scattering profiles of mass fractal objects exhibit power-law behaviour as shown by

$$I(q) = q^{-x} \tag{3}$$

The power-law exponent x is useful in distinguishing between mass and surface fractals because it can be directly related to fractal dimensions. It is very important to note, however, that the power law does not necessarily predict a certain kinetic growth model, which must be developed independently.

Particularly relevant here is small-angle X-ray scattering (SAXS), which is a technique for studying structural features of colloidal size[24–28]. Any scattering process is characterized by a reciprocity law, which gives an inverse relationship between the particle size and scattering dimension. The scattered intensity, $I(q)$, is characterized by the scattered wave vector or momentum transfer q, which for elastic scattering is proportional to $\sin(\theta/2)$, where θ is the angle of scattered intensity relative to the incident beam. The entire equation is

$$I(q) = 4\pi \int_0^\infty \rho(r)[\sin(qr)/qr]\, \mathrm{d}r \tag{4}$$

Solving the above integral indicates that $I(q)$ is proportional to $\Delta\rho$, which is the difference in electron density. Therefore, for small-angle X-ray scattering to occur, there must be a difference in electron density within the system.

A major task in the understanding of disordered systems is recognizing the role of structural features in a small-angle scattering profile. A connection exists between the length scales of a material in real space and how this unfolds in reciprocal space as measured in a scattering experiment. When deducing size, shape or mass from a scattering curve, one has to find a model particle which is 'equivalent in scattering' with the particle in question[24]. Usually, this requires considerable trial and error and can be difficult. It is possible, however, to obtain a number of parameters directly from the scattering curve without the ambiguity of trial and error if one understands the various regimes in the curve[24].

In a typical scattering curve for a two-phase disordered system, the intensity is independent of q at low q. This indicates uniformity on large-length scales. Scattering in this region can be beyond the scope of small-angle X-ray scattering experiments and should then be resolved by light scattering. Increase in q leads to the Guinier regime, where the scattered intensity is no longer independent of q. The dependence on q in this regime is a measure of the size of the particles or, more specifically, the radius of gyration R_g (which is taken as the root-mean-square of the distances of all electrons to their centre of gravity). Guinier's Law, which can be written as

$$I(q) = NV_p\Delta\rho^2 \exp\left(-q^2R_g^2/3\right) \tag{5}$$

can thus be used to determine the R_g of a particle.

Guinier's Law is exact in the limit as q approaches zero and is usually quite accurate in the range $0 \leq q \leq 1/R_g$. The scattered intensity at zero angle [I_0 or $I(0)$] is obtained by extrapolation to $q = 0$, and gives information about the number of particles N present in the system:

$$I_0 \propto NV_p^2\Delta\rho^2 \tag{6}$$

If the system is monodisperse and the difference in electron density is constant, the intensity at zero angle scales as a function of the number of particles in the system. In the case where the system is polydisperse, the radius of gyration and the intensity at zero angle scale as a Z-average of all of the particles in the system; if a dispersity factor is known, it can be related back to a weighted average.

In the following Porod regime, the concept of fractal geometry is very important because structures on these scales are often fractal[20]. Scattering in this regime depends on the geometric structure of the particles in the system. For example, in a log–log plot of the scattered intensity *versus* q, the slope would equal -2 for a random-walk, linear polymer and -3 for a uniformly dense object[29,30]. This power-law behaviour is independent of both the size and short-range chemical details of the scattering particles. However, since there are important differences between the scattering profiles of surface and mass fractals, different equations must be used to calculate the fractal dimensions from the scattering data[18]. As a result, the power-law dependence of the intensity in the Porod regime can be described as[20]

$$I(q) = q^{D_s - 2D_e} \tag{7}$$

The quantity $D = D_s - 2D_e$ is referred to as the Porod slope. For a system composed of particles obeying equation (2),

such as uniformly dense objects, $D_e = 3$ (Euclidean dimensions) and equation (7) becomes

$$I(q) = q^{D_s - 6} \tag{8}$$

In this case, the object is uniform and scattering from the bulk is parallel to the incident beam. The case where $D_s = 2$ (and thus $D = -4$) corresponds to Porod's Law, which is used in characterizing dense objects with smooth surfaces. A rough surface corresponds to $2 < D_s < 3$, resulting in a power-law exponent in the range $-3 < D < -4$. Such fractal dimensions correspond to compact objects with rough surfaces.

If a system is composed of scatterers that more closely follow equation (1), then

$$I(q) = q^{-D} \tag{9}$$

Thus, if the structure is connected (i.e. not a collection of separated regions), the mass fractal dimension is measured directly from the slope of the scattering profile. The case where the Porod slope is less than -4 corresponds to a diffuse interface between the particles and the matrix in which they are embedded.

EXPERIMENTAL

Materials

The PDMS used was obtained from Huls America, and had a quoted value of number-average molecular weight (M_n) of 18 000 g mol^{-1}. Actual values of M_n, weight-average molecular weight (M_w) and polydispersity index (M_w/M_n) were obtained with a Waters 746 gel permeation chromatography instrument. The results were 15 600 g mol^{-1}, 27 900 g mol^{-1} and 1.79, respectively[31]. Tetraethoxysilane (TEOS) [$Si(OEt)_4$] used in the crosslinking reactions was provided by the Aldrich Chemical Corporation and was at least 99.999% pure. The TEOS used as the ceramic precursor was obtained through Huls America, and was at least 99% pure. Titanium n-butoxide (TBO) [$Ti(OBu)_4$], toluene, methanol, hydrochloric acid and diethylamine were also supplied by Aldrich, and stannous *n*-octoate was supplied by the Pfaltz and Bauer Company. All of these materials were used as received.

Preparation of the filled PDMS networks

Preparation of the networks. The networks investigated were prepared from hydroxyl-terminated PDMS by endlinking reactions using TEOS[31]. In this method of network preparation, the molar mass between crosslinks is known, as is the distribution of molar masses and the functionality of the crosslinks. All of the PDMS networks thus prepared were swollen in toluene for 3 days to remove the sol fractions, and were then deswollen in a series of methanol/toluene mixtures, increasing the portion of methanol until the mixture was 100% methanol. The samples were then dried to constant weight and the amount of soluble material determined. This was done by using the differences in weight of the sample before and after extraction with the toluene. The sol fractions were found to be 4–7%.

General aspects of the sol–gel approach. Although there are a number of ways to use the sol–gel technique to prepare hybrid organic composites[1–6, 32–35], the method chosen here was that of 'sequential' processing. Using the preparation of a PDMS/SiO_2 composite as an example, the first step was the already-described formation of an unfilled PDMS network by TEOS endlinking. The next step involved swelling the extracted polymer network in a ceramic precursor, in this case TEOS. This was followed by an acid-catalysed or base-catalysed hydrolysis, and condensation of the precursor to generate the reinforcing filler *in situ*, in this case silica. The overall reaction is shown by the equation

$$Si(OEt)_4 + 2H_2O \rightarrow SiO_2 + 4EtOH \tag{10}$$

The analogous reaction for the *in situ* generation of titania from TBO is

$$Ti(OBu)_4 + 2H_2O \rightarrow TiO_2 + 4BuOH \tag{11}$$

This technique is also referred to as a 'one-step' sol–gel approach[27,28] because, in the conversion of the liquid precursor into a ceramic phase, either an acid or a base catalyst is used for both the hydrolysis and condensation steps.

Preparation of precursor solutions. Since silicon alkoxides are extremely slow to hydrolyse compared with titanium alkoxides, it is not possible to simply hydrolyse a mixture of these two alkoxides; this leads to the two separate oxides. For this reason, starting solutions of ceramic precursors for the silica–titania mixed-oxide filler were prepared by partially reacting the slower TEOS with some TBO[31,36]. TEOS is immiscible with water, necessitating use of a common solvent for its controlled hydrolysis. For this reason, an aqueous HCl solution (pH = 1) was first mixed with ethanol and then with TEOS in the following ratios: TEOS/ethanol/HCl/water = 1/2/0.002/1–1.3. This solution was then allowed to react for 2 h at 65°C under reflux, giving some soluble, partially hydrolysed ethoxysilanol species which can react further by condensation of the silanol portions with other alkoxy groups[31]. Of particular interest was the possible preparation of mixed oxides, i.e. molecules with Si–O–Ti bonding such as $(EtO)_3Si–O–Ti(OBu)_3$. This was attempted by introducing TBO, with vigorous stirring, into the refluxed acidic solutions of TEOS and water in ethanol. This was done using a mole ratio of silicon to titanium of 3:2. ^{29}Si nuclear magnetic resonance spectroscopy (n.m.r.) showed that most of the species obtained in the final liquid precursor have no more than two bridging oxygens, although further polymerization is, of course, possible. This solution was then ready to be used in subsequent sample preparations.

In situ precipitation of silica–titania mixed oxides. The *in situ* precipitation of the silica–titania oxide within the PDMS network was carried out as follows. Sheets of extracted PDMS networks were weighed and then immersed in the precursor solution for various amounts of time[31]. The amount of time the PDMS sheet was allowed to remain in the precursor solution determined the amount of precursor solution absorbed, and the weight percent of filler subsequently generated. The PDMS networks, swollen with the ceramic precursor, were then placed into an aqueous solution of 2 wt% diethylamine basic catalyst (pH = 12). The hydrolysis and condensation of the precursor were allowed to take place for 24 h at room temperature. The sheets were then removed and dried under vacuum. The sheets were then reweighed, and the increases in weight used to calculate the amounts of filler introduced.

In situ precipitation of titania. The procedure for the titania-filled samples was identical to the procedure for the mixed-oxide samples outlined above, except that the swelling precursor was TBO[31].

In situ precipitation of silica. The procedure for the silica-filled samples was identical to those already described, except that the swelling precursor was pure TEOS[31].

SAXS measurements

The small-angle X-ray scattering data were obtained at the University of Cincinnati and at Oak Ridge National Laboratory (ORNL)[31]. The scattering studies at the University of Cincinnati were performed in the Department of Materials Science and Engineering laboratories, using an Anton–Parr Compact Kratky Camera which has a completely evacuated beam path. Cu K_α line radiation ($\lambda = 1.542$ Å) was obtained from a Rigaku 12 kW rotating-anode generator operated at various power settings, with a copper target and graphite monochromator. Scattering curves were recorded at slit settings ranging from 20 to 50 μm at a sample-to-detector distance of 241 mm, using a TEC model 205 one-dimensional position-sensitive proportional counter with a resolution of 47 μm. Sample scattering data were corrected for detector sensitivity, linearity and sample transmission. The sample transmission and the incident X-ray flux were measured with a moving-slit device described by Stabinger and Kratky[37]. The intensity at zero angle was normalized by the incident flux to correct for variations in beam intensity.

The X-ray data from ORNL were obtained with the 10 m small-angle X-ray facility. Cu K_α line radiation that had been graphite-monochromatized was used as the incident wavelength (in an evacuated beam path), with a fixed beam size at the specimen chamber of 0.1 cm $\times$ 0.1 cm. Data were collected at sample-to-detector distances of 5.126 and 3.126 m. The scattering patterns were detected by a two-dimensional position-sensitive proportional counter with a 20 cm $\times$ 20 cm active area and the potential for 200 $\times$ 200 resolution elements.

Stress–strain measurements

Equilibrium stress–strain isotherms on samples relevant to this study have been reported elsewhere[15,16]. They were obtained on unswollen strips at room temperature, in the usual manner[31,38–40]. Specifically, the sample strip was mounted between two clamps, with the lower clamp being fixed, with both lined with thin sheets of rubber to prevent slippage of the sample. The upper clamp was fastened to a moveable stress transducer (Statham model # G 1-16-350). The transducer was calibrated with a standard set of weights, and the output was monitored by a Leeds and Northrup Speedomax recorder.

The edge of a razor blade, coated with carbon black, was used to mark two lines on each sample[15,16]. The length of the sample was measured precisely, using the marked lines, by means of a Gaertner Scientific Corporation model M940-303P cathetometer with a precision of $\pm$ 1 μm. The average undeformed cross-sectional area, A^*, was determined by measuring the thickness and width of each sample with a micrometer.

When the transducer output, or stress, no longer changed discernibly with time, the force was recorded and the strain was increased for the next data point. The stress–strain measurements were taken in the direction of increasing elongation and carried out to the rupture points[15,16].

The reduced stress was calculated from the equation[38–40]

$$[f^*] \equiv f^*/(\alpha - \alpha^{-2}) \qquad (12)$$

where $f^* \equiv f/A^*$ is the nominal stress, f the equilibrium force, and $\alpha \equiv L/L_i$ the elongation (length of the sample, L, relative to its initial length, L_i).

Kinetics experiments

Silica–titania mixed-oxide/PDMS composites. A series of SAXS experiments was designed to follow the formation and growth of the silica–titania filler particles within the PDMS network over time[31]. This was done to help develop a model for the growth mechanism of the reinforcing particles. In this part of the research, 20 samples in total were prepared by the procedures outlined above, with the following exceptions. The thickness of the PDMS sheets was approximately 0.25 mm, and all sheets were swollen for 20 min in the precursor solution. The times the samples were in the 2 wt% diethylamine solution were varied over 24 h, in order to follow the *in situ* reaction. After the prescribed time in the hydrolysis solution, the samples were sealed in bags of polyethylene, a relatively low-intensity scatterer, and the scattering profiles were recorded. Additionally, samples were tested to see if the hydrolysis and condensation reactions continued after removal from the catalyst solution. The samples showed no further reaction. Therefore, upon removal of a sample from the solution, the reaction was essentially quenched and such samples removed at regular intervals could be reliably tested later. This considerably simplified things, since wet samples could have caused damage to the SAXS instrument, which operates under high vacuum.

Titania/PDMS composites. A series of titania-filled PDMS samples was prepared following the previously outlined procedures, with the following exceptions[31]. The thickness of the PDMS sheets was approximately 0.25 mm, and all sheets were swollen for 15 min in the precursor solution. The amount of time the samples were in the 2 wt% diethylamine solution was varied over 24 h, as already described.

Silica/PDMS composites. The exceptions in this case were that the thickness of the PDMS sheets was approximately 0.25 mm, and all sheets were swollen for 30 min in the precursor solution[31]. The amount of time the samples were in the 2 wt% diethylamine solution was again varied over 24 h, as already described.

RESULTS AND DISCUSSION

Synthesis and structure

Silica–titania/PDMS composites. The incorporation of the co-silica–titania phases into the PDMS networks was originally believed to follow the four-part reaction scheme shown below[31].

(a) Partial hydrolysis of TEOS in acid:

$$Si(OEt)_4 + H_2O \rightarrow Si(OH)(OEt)_3 + EtOH \qquad (13)$$

Calculations performed using a binomial distribution showed that only 42% of the product will actually be that shown, however, since there is a distribution of silanol species. Twenty-one per cent of the product will be of the form $Si(OH)_2(OEt)_2$, 5% will be $Si(OH)_3(OEt)$, less than 1% $Si(OH)_4$, and 32% will be unreacted TEOS. Use of the binomial distribution requires the assumption that water is equally likely to react at any ethoxy site (i.e. either the event—a site reacts—occurs or the event does not occur). This is not completely accurate as the rate for each subsequent site to hydrolyse is not the same, but the

approximation is reasonable enough. Therefore, the calculations do serve the purpose in emphasizing that a distribution of products should be expected.

(b) Reaction of the silicate products from (a) with TBO:

$$(OEt)_3Si–OH + BuO–Ti(OBu)_3 \rightarrow (OEt)_3Si–O–Ti(OBu)_3 + BuOH \quad (14)$$

^{29}Si-n.m.r. shows that this ceramic precursor is made up mostly of Q^0 and Q^1 species with some Q^2 and very little Q^3 species (where Q corresponds to species with a functionality of four and the superscript represents the number of bridging oxygen atoms). However, diffuse reflectance Fourier transfrom infra-red (*FT*i.r.) spectra[41] confirm the presence of Si–O–Ti bridges, at least temporarily, as monitored by a characteristic 945–960 cm^{-1} vibration.

(c) Further hydrolysis of the product from (b) in base:

$$(OEt)_3Si–O–Ti(OBu)_3 + \text{excess } H_2O \rightarrow (OH)_3Si–O–Ti(OH)_3 + 3BuOH + 3EtOH \quad (15)$$

(d) Subsequent condensation:

$$n(OH)_3Si–O–Ti(OH)_3 \rightarrow n(–O–Si–O–Ti–) + 3n/2H_2O \quad (16)$$

It is well known that the resulting structures of sol–gel reaction products involving hydrolysis and condensation of metal alkoxides are very dependent upon the reaction conditions. Several factors are known to affect the structures, including alkyl group substitution[42], catalyst[43], pH[43], temperature[44], water concentration[45] and reaction time. All of the reaction conditions tend to lead the structural development along a particular mechanistic pathway[46]. For example, small-angle scattering experiments conducted by Schaefer and Keefer[47] on the polymerization of silicon alkoxides show that acid catalysis leads to polymeric-type structures, as the reaction product is only weakly crosslinked. This type of structure results when substoichiometric amounts of water are used. Conversely, base-catalysed systems generally yield denser, colloidal structures, as do reaction conditions with a large excess of water.

With these ideas in mind, SAXS measurements were performed on two of the samples reinforced with silica–titania, and on one reinforced with titania. The mixed-oxide samples contained 15.8 and 21.4 wt% of filler and the titania sample had 19.3 wt% filler. The samples were scanned for 1000 s with instrument power settings at 40 kV and 40 mA. The scattering curves from the ORNL are shown in *Figures 1 and 2*. Analysis of the plots showed a decade of power-law behaviour corresponding to a Porod slope of -3.5 to -3.6 for all samples. Slit-smeared data from the University of Cincinnati gave scattering exponents of -2.6 for the mixed system and -2.5 for the titania system. In a slit-smeared experiment, the scattering exponents scale differently than in pin-hole collimated beam experiments[24], there being a difference of 1. That is,

$$D_{\text{slit–smeared}} = D + 1 \quad (17)$$

In other words, a slit-smeared exponent of -2.5 corresponds to an exponent of -3.5 for X-ray scattering done with pin-hole collimation. Therefore, the two systems exhibit good agreement. This power-law behaviour implies that the filler structure in the two samples is similar. The Porod slope suggests the presence of compact, particulate fillers. They are therefore maximally rough colloids and/or maximally dense polymers. This agrees with previous work on the hydrolysis of metal alkoxides (specifically of silicon and titanium) in a basic medium[14].

Analysis of the Guinier region of the samples shows a difference in average particle size. The 15.8 wt% mixed-oxide sample has a radius of gyration of approximately 155 Å, whereas the 21.4 wt% mixed-oxide sample has a value of 170 Å. The titania sample exhibits an R_g of 110 Å. Additionally, there is some evidence of secondary maxima in the scattering curve in the crossover region between the Guinier and Porod regimes. This could indicate that the particles are at least approximately spherical and very nearly monodisperse; however, as Rodrigues *et al.*[48] have previously pointed out, without treatment of the data for thermal density flucuations, these results are more indicative of the trends reported here (which are believed to be sound). The reader is cautioned that the quantative accuracy may be less due to the neglection of treating possible thermal density fluctuations.

At the end of the Porod regime, at very high angles, there is a low-intensity plateau which seems to exhibit a peak. According to Kallala *et al.*[49], if the ratio of H^+ to Ti is very low (as in a base-catalysed reaction), this peak indicates that the coordination number of titanium becomes substantially larger than 2. Accordingly, the local structure of polymers made at low H^+-to-Ti ratios also appears to be dense.

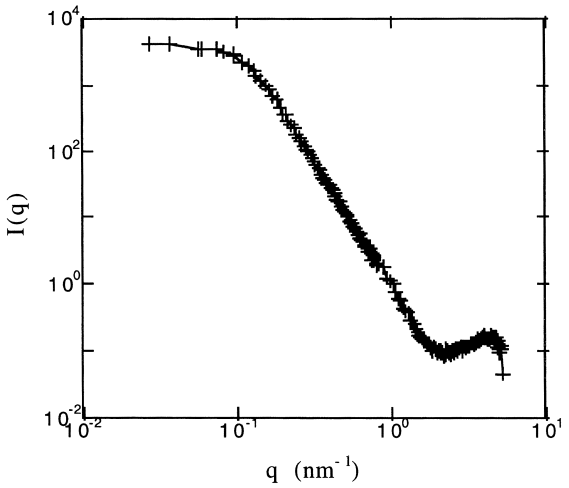

Figure 1 SAXS profile for a 15.8 wt% SiO_2–TiO_2/PDMS composite

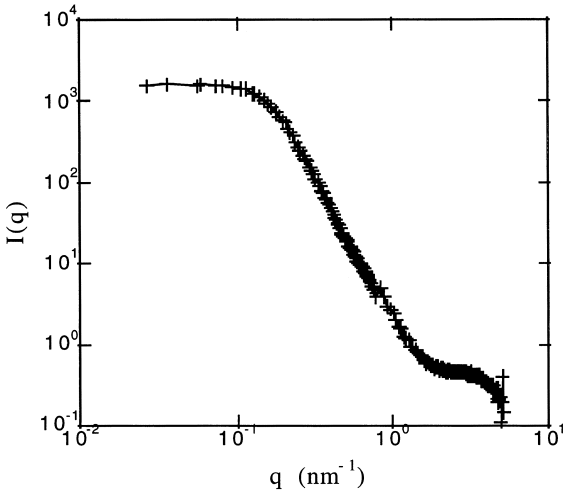

Figure 2 SAXS profile for a 19.3 wt% TiO_2/PDMS composite

Titania/PDMS composites. The scattering curve for the titania sample is very similar to those for the mixed-oxide system, except that the high-angle plateau does not have a peak but instead crosses over into another Gaussian regime[31]. Attempts to characterize this regime yielded no meaningful information.

Kinetic experiments

Silica–titania/PDMS composites. The first series of samples consisted of silica–titania-reinforced PDMS, in which the samples had been swollen in the alkoxide solution and then put into the basic hydrolysis solution for varying periods of time (from minutes to tens of hours). SAXS data collected on this series show the formation of particles after as little as 2 min exposure in the catalyst solution, and the radius of gyration quickly approaches 90 Å. It continues to increase, but not by much more than 10% during the first hour. Thereafter, it remains unchanged, within experimental error, for the next 8 to 9 h. After 9 h, the radius of gyration starts to increase by an amount larger than the experimental uncertainty. Over the course of the final 6 to 8 h of the experiment, the radius of gyration of the samples appeared to level off at approximately 135 Å. The dependence of the R_g in this system on time is shown in *Figure 3*. Within an hour, the Porod region of the scattering curve consistently shows a slit-smeared exponent of -2.5, corresponding to a power-law slope of -3.5. At longer times the exponent may approach -3.6, but this difference is within experimental error. These exponents agree with the exponent from the 15.8 and 21.4 wt% mixed-oxide samples. Therefore, it is concluded that this system quickly develops compact particulate fillers with fractally rough surfaces.

One of the most interesting observations is that the intensity at zero angle increases throughout the entire experiments. Since $I(0)$ is proportional to the number of particles in a system and to their size, this increase means that during the first 6 to 8 h of the experiment (where the radius of gyration remains essentially constant) the number of nucleation sites, and thus the number of particles, is increasing. *Figure 4* shows the time dependence of $I(0)$, in which $I(0)$ is normalized by the incident flux to correct for variations in the incident beam intensity.

The fact that the number of particles increases with time is consistent with the time involved for diffusion of water into the polymer network. Since water is required for hydrolysis of the precursor solution, this corresponds to the time it takes water to diffuse into the interior of the sample for these reactions to occur. Over the final 10 h, the intensity at zero angle increases only slightly. This is most likely due to an increase in the sizes, and thus the volumes, of the particles.

With this information in hand, it was possible to propose two models to possibly explain the two-part growth patterns observed, i.e. the almost immediate formation of particles and their continued growth over time. The first model assumed a titania-rich core with the silica forming later to further densify the particles and to increase their size. This model is very unlikely, however, because titanium has a tendency to be in higher coordinations (i.e. octahedral). As a result, titanium tends to be segregated such that it is surrounded solely by other titanium atoms. Silicon, on the other hand, favours tetrahedral coordination. These characteristics are in agreement with the scattering peaks at large angles that correspond to higher coordinations.

The second model proposed suggests that two distinct sets of particles are formed. That is, titania and silica particles are formed nearly independently. This would be in contrast to the chemistry of the mixed-oxide precursor solution, where diffuse reflectance *FT*i.r. confirms the existence of Si–O–Ti bonds, at least temporarily. In fact, Dire *et al.*[50] showed that, in solution, evolution of the hydrolysis and condensation process can proceed through the formation of Si–O–Ti bonds, but structural rearrangements lead to Si–O–Si and Ti–O–Ti bonds. Additionally, Aizawa *et al.*[51] concluded that at high pH, Si–O–Si bonds are energetically favoured over Si–O–Ti bonds. During condensation in a basic medium, Si–O–Ti bonds cleave, forming domains rich in Ti–O–Ti and Si–O–Si. Finally, Chmel *et al.*[52] state that in the formation of glasses, a SiO_2–TiO_2 glass is unstable if the content of titanium is greater than 8 mol%. In the present system, based upon the 6:4 mole ratio of silicon to titanium, titanium accounts for approximately 28 mol% of the elements present (i.e., titanium, silicon and oxygen).

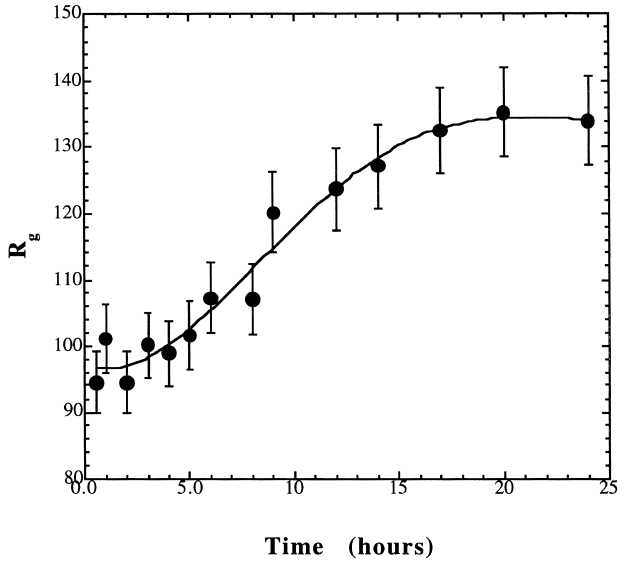

Figure 3 The radius of gyration as a function of time for the SiO_2–TiO_2/PDMS composite

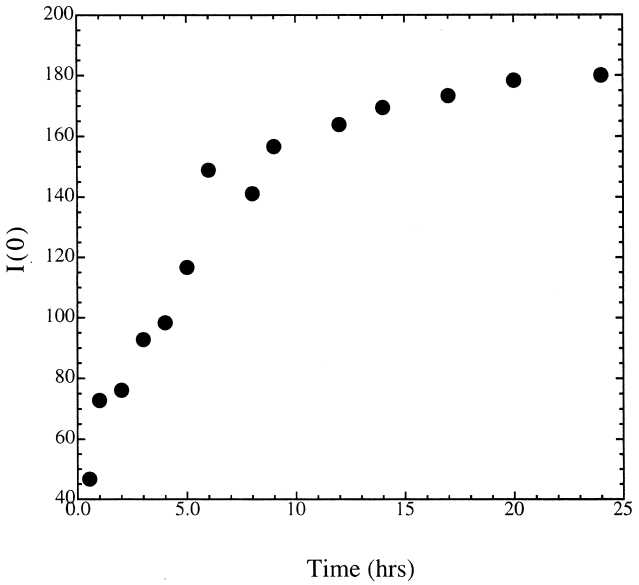

Figure 4 The normalized intensity at zero angle as a function of time for the SiO_2–TiO_2/PDMS composite

Therefore, a series of hypotheses was made to further describe the second model. Upon addition of a PDMS precursor-swollen network into the diethylamine solution, there is immediate formation of TiO_2 particles, and the particle size rapidly approaches a constant value. Since $I(0)$ is proportional to the number of particles, this indicates that the number of particles continues to increase with time as water diffuses into the polymer network. The formation of SiO_2 proceeds at a much slower rate. Therefore, the water that is diffusing into the network will 'choose' to react with any Ti–OH or Ti–OR species (where R is an alkyl group) before reacting with any silicon species. Essentially, this means that before any of the silicon species can react, the titanium species' reactions could be nearly exhausted. After 6 to 8 h, however, the number of silica particles is significantly large, their size may exceed that of titania, and the scattering intensity due to the silicon becomes comparable to that from the titanium. Scattering intensity is directly related to the number of electrons of an atom in a species, and atoms of increasing atomic number are therefore more intense scatterers. In a mixed system, the scattered intensity is a result of a weighted average so that, as the amount of silica in the system increases, the data should begin to reflect this.

Separate titania/PDMS composites. Two series of TiO_2-reinforced PDMS and SiO_2-reinforced PDMS samples were used to test the latter model. Separate SiO_2 and TiO_2 kinetic SAXS experiments should elucidate the growth mechanisms in the mixed-oxide systems.

The SAXS from the titania samples was measured, and showed the immediate formation of particles. After just 2 min in the hydrolysis solution, titania particles exhibiting an R_g of approximately 50 Å had formed. After 30 min, the radius of gyration approaches 75 Å and finally after 1 h the radius of gyration reaches a near-constant value. From 1 h up to 20 h, R_g remains around 100 ± 10 Å. This dependence of the radius of gyration on time is shown in *Figure 5*.

The intensity at zero angle is very important in this set of experiments, and is illustrated in *Figure 6*. $I(0)$ increases for the first 5 to 7 h and then remains constant. Since the radius of gyration is constant for times greater than 1 h, the increase in $I(0)$ is consistent with an increase in the number of particles. The lack of change in $I(0)$ after 5 to 7 h indicates that essentially all of the TBO in the network has reacted, forming TiO_2. Therefore, in the case of formation of titania particles, the reaction is complete by this time.

As can be seen from *Figure 7*, the Porod slope for the TiO_2/PDMS composite exhibits no further changes after 1 h of reaction in the basic hydrolysis solution. The first sample, which was allowed to react for 2 min, has a power-law slope of − 2.7 (corresponding to a mass fractal dimension of the same value). The reaction between the TBO and water was immediate and the initial structure of the titania filler was similar to a highly branched polymer chain. After 30 min in the solution, the sample shows a slope approaching − 3.2. The filler particles have had sufficient time to densify their structure and are now compact particles. While they have not yet grown as dense as in the final structure, they have begun to show signs of the ultimate structure they will achieve. After 1 h, the slope becomes constant, suggesting that no further changes in structure were taking place.

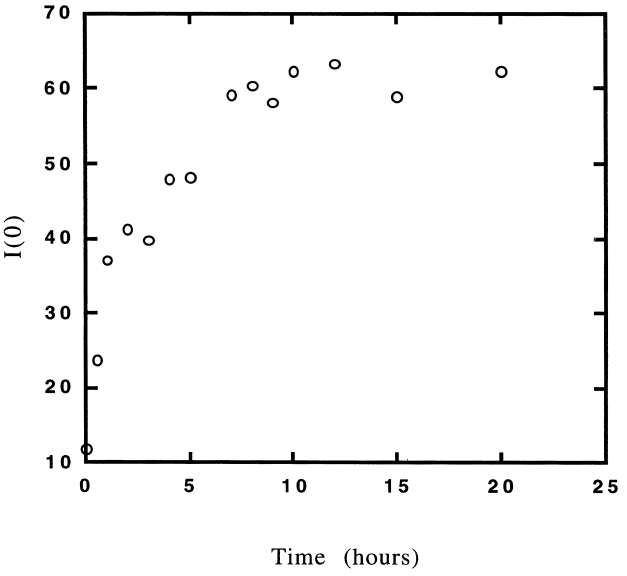

Figure 6 The normalized intensity at zero angle as a function of time for the TiO_2/PDMS composite

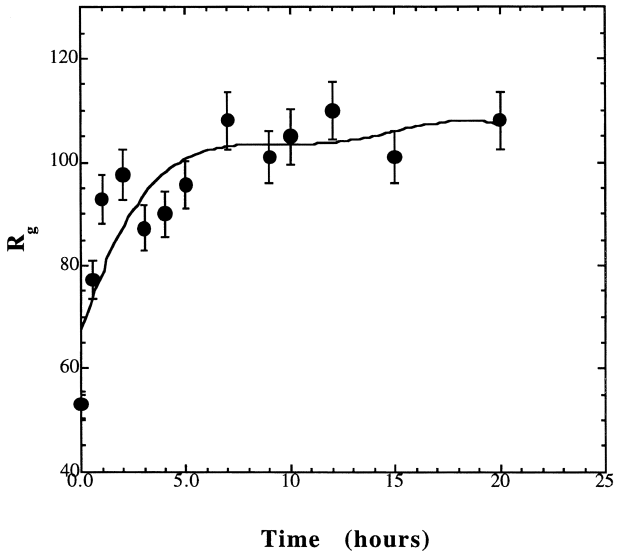

Figure 5 The radius of gyration as a function of time for the TiO_2/PDMS composite

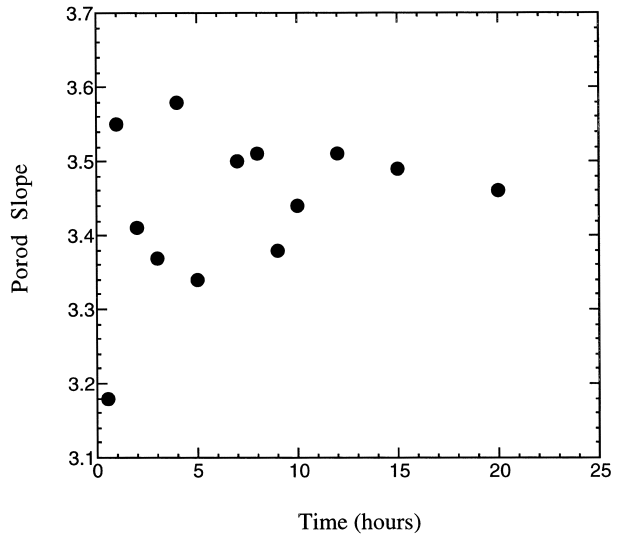

Figure 7 Porod exponent as a function of time for the TiO_2/PDMS composite

These results can be accounted for as follows. When the samples are placed into the hydrolysis solution, water reacts with the TBO near the surface, forming titania particles and butanol. Because of the butanol, water is able to diffuse into the swollen PDMS network which otherwise is hydrophobic, and the TBO is hydrolysed immediately into particles. Since diffusion of the alkoxides into the network is slower than particle growth, the depletion of the precursor by an existing titania particle inhibits nucleation of a nearby particle, and the particle size is determined by the amount of TBO in the immediate vicinity of the particle. The particles are thus relatively uniform in size, accounting for the suggestion of secondary maxima in the scattering curves. They are also uniformly, rather than randomly, dispersed throughout the network. As the water diffusion front advances into the elastomer, more titania particles precipitate, but their size remains essentially constant. This would account for the increase in $I(0)$, in spite of the constancy of the radius of gyration. The PDMS network effectively 'poisons' growth sites on the titania particles, thereby generating a fractally rough surface similar to that in the poisoned-Eden model developed by Keefer (with a surface fractal dimension of 3.5)[53].

All the pure titania samples showed a crossover into another Gaussian regime. This could indicate that surface roughness extends to the smallest possible dimensions. In this interpretation, the titania particles are probably porous and surround the PDMS chains owing to the nature of the growth processes. That is, the growth of the particles is sufficiently fast so that they will grow around any PDMS chains they may encounter. Because of the size of the particles ($R_g = 100$ Å) relative to the estimated distance between crosslinks (10–20 Å), this is an extremely likely possibility.

Separate silica/PDMS composites. The SAXS from these samples indicated that the formation of silica particles in the PDMS networks is much slower than the formation of titania under similar reaction conditions. Samples removed after anywhere from 30 min up to 3 h in the hydrolysis solution exhibited little or no particle formation. The first sample to give reasonable statistics (i.e. counts per second by the detector) that were consistent with the formation of particles was the 4 h one. It showed an R_g of 110 Å, which indicates that nucleation of silica particles is most likely the rate-determining step. There was no significant formation of particles at 3 h and an hour later there were rather large particles present, showing that once nucleation of a particle has begun, its initial growth is rather rapid. The radius of gyration continued to become larger throughout the entire experiment although it shows signs of levelling off during the latter stages. The radius of gyration as a function of time in the SiO_2/PDMS composite is shown is *Figure 8*.

Values of the Porod slope as a function of time[31] indicated that the silica particles at 4 h had a surface fractal dimension of 3.6. This is a sign that the particles immediately form a dense structure under these conditions. At 5 h, the slope had further decreased to -3.8 and the 7 h sample exhibited a slope of -3.9. After 7 h, the slope remained fairly constant at 3.9 ± 0.1. This indicated that the structure of the silica was that of a dense particulate, and additionally showed signs of a smooth surface, signified by the fact that the power-law exponent approaches -4 (i.e. Porod's law).

The intensity at zero angle as a function of time is shown in *Figure 9*. $I(0)$ increases throughout the entire experiment, which indicates that either the number of nucleation sites or the sizes of the particle, or both, increase during this time. Keefer[12] conducted studies on the formation of silica by similar processes in solution. He showed that if a supply of TEOS is continuously available for the formation of silica, then the particle size will continue to increase. This process is known as chemically limited growth. In these processes, the probability of a monomer attaching itself to a cluster is small with respect to the number of encounters that monomer may have with an available reacting site. All potential growth sites are therefore sampled by the monomers. The probability for attachment is determined by local structure, which determines the probability of attaching to a particular site per encounter. This is in contrast to the large-scale structure (which governs the probability that a monomer will encounter a given site) which represents a diffusion-limited process. The fact that the radius of gyration in this system grows rapidly upon nucleation coincides with chemically limited growth theory.

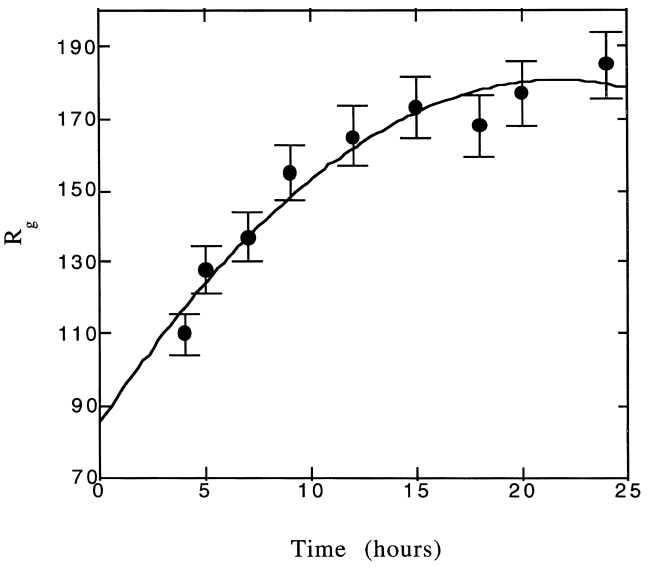

Figure 8 The radius of gyration as a function of time for the SiO_2/PDMS composite

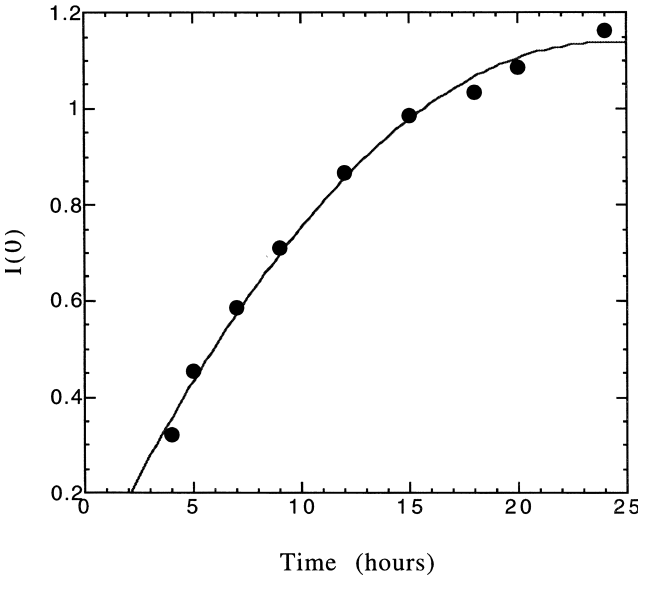

Figure 9 The normalized intensity at zero angle as a function of time in the SiO_2/PDMS composite

Upon nucleation, the frequency of encounters is very large, due to the number of monomers available, and thus the probability of attachment is high. As the monomers react, the frequency of encounters decreases, thus decreasing the speed of particle growth.

Chemically limited growth, or reaction-limited growth by monomer–cluster type addition, yields the type of dense particulates found in all of the systems studied. Specific to the silica system, however, is the conclusion that the increase in $I(0)$ is mostly due to an increase in the particle size as time increases. This is based on the conclusion that the growth is chemically limited, along with the fact that the radius of gyration and the intensity at zero angle increased similarly during the kinetic experiments. At early times in the SiO_2/PDMS kinetic experiments ($< 5–7$ h), the number of particles increases rapidly as water diffuses into the PDMS network and nucleation of the particles takes place. It is safe to assume that after a large number of particles have nucleated, the increase in $I(0)$ must therefore be due to the observed increase in particle size. Additionally, as the radius of gyration becomes constant at longer times (approaching 24 h), the intensity at zero angle begins to level off, also indicating that no further nucleation is taking place. This is also an indication that all or nearly all of the available monomer has reacted, preventing additional growth of the particles.

Mechanical properties

Mechanical properties of the titania/PDMS composites. In order to determine the relationship between the structure of titania particles and their effect on the mechanical properties of a TiO_2/PDMS composite, reference is made to some equilibrium stress–strain measurements that have been reported for a composite containing 19.5 wt% titania. These isotherms, in terms of the reduced stress as a function of reciprocal elongation[38–40], are shown in *Figure 10*[15,16].

Compared with the unfilled PDMS network, the TiO_2-reinforced PDMS network shows a considerable increase in strength. An increase in reduced stress of approximately 18-fold is apparent at small elongations, while a five- to six-fold increase is obtained at higher elongations. Additionally, a significant increase in the elongation at break is obtained relative to the pure PDMS network. The unfilled network ruptures at slightly more than 100% elongation, whereas the TiO_2/PDMS composite ruptures at an elongation of nearly 250%.

Compared with an SiO_2/PDMS composite with a similar amount of reinforcing filler (22.4 wt%), the TiO_2/PDMS composite shows better reinforcement at small elongations (less than 30%)[15,16]. On the other hand, the TiO_2/PDMS composite does not exhibit the upturn in the modulus that is apparent in the silica-reinforced system, but once again shows a significant improvement in the elongation at break.

These mechanical properties of the TiO_2/PDMS composite can possibly be explained by the fractally rough surface and porous nature of the titania particles, resulting in good mechanical bonding of the particles to the PDMS network[31].

Mechanical properties of the silica–titania/PDMS composites. The relevant isotherms here are those reported for a silica–titania/PDMS composite containing 21.4 wt% filler. They are also shown in *Figure 10*[15,16].

Compared with an unfilled PDMS network, the PDMS network reinforced by the mixed oxide shows a very large increase in strength. An increase of over 200% is achieved at small elongations, and a 15-fold increase near the rupture point. The elongation at break is slightly better than for the unfilled system, but probably (given the experimental error) they are equivalent. Compared with the 22.4 wt% SiO_2/PDMS composite, the mixed-oxide one exhibits better reinforcement effects throughout the entire range of elongations. There is also a marked increase in the elongation at break relative to the silica-reinforced PDMS. The mixed-oxide system also shows better properties than those exhibited by the TiO_2/PDMS composite[15,16]. It has a higher modulus at low elongations, and shows an upturn in modulus at higher elongations not shown by the titania-reinforced system.

The mechanical properties of the mixed system can be explained as follows. The titania particles in this system provide the same type of reinforcement they do in the TiO_2/PDMS composite. They provide excellent reinforcement at small elongations and allow the network additional elongation before break relative to unfilled PDMS or silica-reinforced PDMS networks. The silica particles provide significant reinforcement at all elongations, but specifically they account for the higher modulus at moderate elongations and for the upturns in modulus at high elongations. There is thus a very useful 'delegation of responsibilities' in this mixed-oxide system. The silica particles are able to provide good reinforcement at high elongations in part because they are randomly dispersed, at least with respect to the titania particles, if not with respect to each other. Also, silica provides this excellent reinforcement due to the existence of an extended bound polymer/filler interface[54,55]. Under strain it contributes an additional force of recovery over that supplied by the polymer network, as well as dissipating the strain energy through internal friction.

According to Edwards[56], optimal reinforcement appears to involve both physical and chemical interactions. Physical factors prevent escape of the polymer from the filler surface (vacuole formation), but allow stress delocalization through interfacial slippage. Occasional stronger bonds may be introduced advantageously to facilitate dissipation of strain energy and optimize properties relating to resilience and durability. However, only a minor amount of strong bonding is necessary or even desirable, such that polymer–filler slippage can occur, under stress, over most of the interfacial area. This provides an increased resistance to premature failure and, because of the reversible nature of the adsorption of PDMS on the filler surface[57], the network would reform (though not necessarily to its original configurations) upon release of the strain.

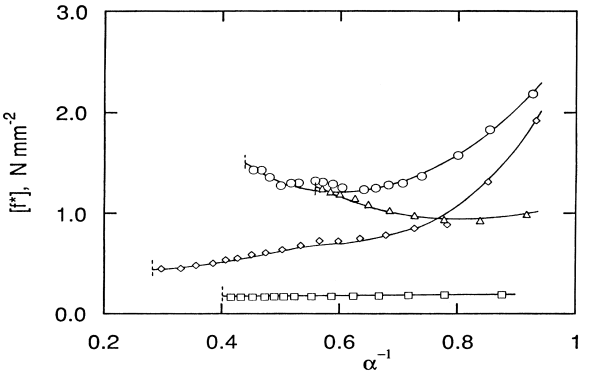

Figure 10 Stress–strain isotherms for PDMS networks filled with silica, titania or mixed silica–titania[15,16]: □, unfilled; △, 22.4 wt% silica; ◇, 19.5 wt% titania; ○, 21.4 wt% silica–titania mixed oxides

CONCLUSIONS

The growth mechanisms of titania and co-silica–titania particles formed *in situ* by base catalysis have been determined, and some of the effects of the resulting structures on mechanical properties have been clarified.

The hydrolysis of the titanium butoxide in a PDMS network proceeds very quickly, forming titania particles, and probably follows the poisoned-Eden model. The PDMS network chains act as poisoning sites, resulting in particulates with fractally rough surfaces as determined by SAXS. At elongations of less than approximately 30% the titania particles, due to their rough surface and growth around the polymer chains, provide good reinforcement. At higher elongations reinforcement from the titania is apparent although it is not comparable to that from either the silica or the mixed oxides. Elongation at break, however, is significantly improved relative to all of the systems investigated.

In the mixed-oxide system, the Si–O–Ti bonds are readily cleaved in basic solution allowing the formation of separate titania and silica particles. The titania particles grow in a fashion similar to, if not exactly the same as, those in the process outlined above. The silica particles grow at a much slower rate. This is partly due to the fact that any molecule containing titanium with an available reactive site will react with water that has diffused into the network before any reactive site on a silicon atom can. Therefore, the formation of titania proceeds to near completion before the formation of silica particles takes place. The silica particles grow very quickly upon nucleation, which appears to be the rate-determining step. The particles are much larger than the titania particles and provide significant reinforcement throughout the entire range of strain, up to rupture. At high elongations, the mixed-oxide system exhibits an upturn in modulus. Additionally, the elongation at break is greater than that of the PDMS reinforced by silica alone.

The PDMS reinforced with mixed-oxide seems to combine the best properties contributed by titania and silica, relative to reinforcement by either set of particles themselves. The titania provides additional reinforcement at low strains and allows for higher elongations to be obtained, whereas the silica contributes to the reinforcement over the entire range of allowable strain, and gives rise to the very desirable upturns in modulus at high elongations.

ACKNOWLEDGEMENTS

It is a pleasure to acknowledge the financial support provided by the National Science Foundation through Grant DMR-9422223 (Polymers Program, Division of Materials Research), and by the Dow Corning–Sandia CRADA Program. Several discussions with Professor G. Beaucage of the University of Cincinnati Department of Materials Science and Engineering are also gratefully acknowledged.

REFERENCES

1. Hench, L. L. and Ulrich, D. R. (Eds.), *Ultrastrucure Processing of Ceramics, Glasses, and Composites*. Wiley and Sons, New York, 1984.
2. Uhlmann, D. R. and Ulrich, D. R. (Eds.), *Ultrastructure Processing of Advanced Materials*. Wiley and Sons, New York, 1992.
3. Novak, B. M., *Adv. Mater.*, 1993, **5**, 422.
4. Mark, J. E. and Calvert, P. D., *Mater. Sci. Eng. C: Biomim. Mater. Sens. Syst.*, 1994, **1**, 159.
5. Mark, J. E., *Polym. Eng. Sci.*, 1996, **36**, 2905.
6. Mark, J. E., *Hetero. Chem. Rev.*, 1996, **3**, 307.
7. Barry, A. J. and Beck, H. N., *Inorganic Polymers*. Academic Press, New York, 1962.
8. Warrick, E. L., Pierce, O. R., Polmanteer, K. E. and Saam, J. C., *Rubber Chem. Technol.*, 1979, **52**, 439.
9. Mark, J. E., Allcock, H. R. and West, R., *Inorganic Polymers*. Prentice Hall, Englewood Cliffs, NJ, 1992.
10. Schaefer, D. W., Mark, J. E., McCarthy, D. W., Jian, L., Sun, C.-C. and Farago, B., *Mater. Res. Soc. Symp. Proc.*, 1990, **171**, 57.
11. Schaefer, D. W., Martin, J. E., Wiltzius, P. and Cannell, D. S., *Phys. Rev. Lett.*, 1984, **52**, 26.
12. Keefer, K. D., *Mater. Res. Soc. Symp. Proc.*, 1986, **73**, 29.
13. Schaefer, D. W. and Keefer, K. D., *Mater. Res. Soc. Symp. Proc.*, 1984, **32**, 1.
14. McCarthy, D. W., Ph.D. thesis, The University of Cincinnati, 1992.
15. Wen, J., Ph.D. thesis, The University of Cincinnati, 1993.
16. Wen, J. and Mark, J. E., *Rubber Chem. Technol.*, 1994, **67**, 806.
17. Mandelbrot, B. B., *The Fractal Geometry of Nature*. Freeman, San Francisco, CA, 1982.
18. Avnir, D. (Ed.), *The Fractal Approach to Heterogeneous Chemistry*. John Wiley and Sons, New York, 1989.
19. Schaefer, D. W., Bunker, B. C. and Wilcoxon, J. P., *Proc. Roy. Soc. London A*, 1989, **423**, 35.
20. Schaefer, D. W., *MRS Bull.*, 1988, **8**, 22.
21. Schaefer, D. W., *Science*, 1989, **243**, 1023.
22. Meakin, P., in *On Growth and Form*, eds H. E. Stanley and E. N. Ostrowsky. Martinus-Nijhoff, Boston, MA, 1986.
23. Schaefer, D. W., *Mater. Res. Soc. Symp. Proc.*, 1987, **79**, 47.
24. Glatter, O. and Kratky, O. (Eds.), *Small-Angle X-ray Scattering*. Academic Press, New York, 1982.
25. Landry, M. R., Coltrain, B. K., Landry, C. J. T. and O'Reilly, J. M., *J. Polym. Sci., Polym. Phys. Edn.*, 1995, **33**, 637.
26. Wignall, G. D., in *Physical Properties of Polymers Handbook*, ed. J. E. Mark. American Institute of Physics Press, Woodbury, NY, 1996, p. 299.
27. McCarthy, D. W., Mark, J. E. and Schaefer, D. W., *J. Polym. Sci., Polym. Phys. Edn.*, 1998, **36**, 1167.
28. McCarthy, D. W., Mark, J. E., Clarson, S. J. and Schaefer, D. W., *J. Polym. Sci., Polym. Phys. Edn.*, 1998, **36**, 1191.
29. Schaefer, D. W. and Curro, J. G., *Ferroelectronics*, 1980, **30**, 49.
30. Porod, G., *Kollid Z.*, 1951, **124**, 83.
31. Breiner, J. M., Ph.D. thesis, The University of Cincinnati, 1996.
32. Mark, J. E. and Schaefer, D. W., *Mater. Res. Soc. Symp. Proc.*, 1990, **171**, 51.
33. Wilkes, G. L., Brennan, A. B., Huang, H. H., Rodrigues, D. and Wang, B., *Mater. Res. Soc. Symp. Proc.*, 1990, **171**, 15.
34. Wei, Y., Bakthavatchalam, R. and Whitecar, C. K., *Chem Mater.*, 1990, **2**, 337.
35. Schmidt, H. K., *Macromol. Symp.*, 1996, **101**, 333.
36. Yoldas, B. E., *J. Non-Cryst. Solids*, 1980, **38/39**, 81.
37. Stabinger, H. and Kratky, O., *Makromol. Chem.*, 1978, **179**, 1655.
38. Treloar, L. R. G., *The Physics of Rubber Elasticity*, 3rd edn. Clarendon Press, Oxford, 1975.
39. Mark, J. E. and Flory, P. J., *J. Appl. Phys.*, 1966, **37**, 4635.
40. Erman, B. and Mark, J. E., *Structures and Properties of Rubberlike Networks*. Oxford University Press, New York, 1997.
41. Schrami-Marth, M., Walther, K. and Wokaun, L. A., *J. Non-Cryst. Solids*, 1992, **143**, 93.
42. Chen, K. C., Tsuchiya, T. and Mackenzie, J. D., *J. Non-Cryst. Solids*, 1986, **81**, 227.
43. Pope, E. J. A. and Mackenzie, J. D., *J. Non-Cryst. Solids*, 1986, **87**, 185.
44. Colby, M. W., Osaka, A. and Mackenzie, J. D., *J. Non-Cryst. Solids*, 1986, **82**, 37.
45. Yoldas, B. E., *J. Non-Cryst. Solids*, 1986, **83**, 375.
46. Keefer, K. D., *Mater. Res. Soc. Symp. Proc.*, 1984, **32**, 15.
47. Schaefer, D. W. and Keefer, K. D., *Phys. Rev. Lett.*, 1984, **53**, 1383.
48. Rodrigues, D., Brennan, A. B., Betrabet, C., Wang, B. and Wilkes, G. L., *Chem. Mater.*, 1992, **4**, 1437.
49. Kallala, M., Sanchez, C. and Cabane, B., *J. Non-Cryst. Solids*, 1992, **147/148**, 189.

50. Dire, S., Babonneau, F., Cartwan, G. and Livage, J., *J. Non-Cryst. Solids*, 1992, **147/148**, 62.
51. Aizawa, M., Nosaka, Y. and Fujii, N., *J. Non-Cryst. Solids*, 1992, **146**, 213.
52. Chmel, A., Eranosyan, G. M. and Kharshak, A. A., *J. Non-Cryst. Solids*, 1992, **146**, 213.
53. Keefer, K. D. and Schaefer, D. W., *Phys. Rev. Lett.*, 1986, **56**, 2367.
54. Galanti, A. V. and Sperling, L. H., *J. Appl. Polym. Sci.*, 1970, **14**, 2785.
55. Arenguren, M., Ph.D. thesis, The University of Minnesota, 1990.
56. Edwards, J. L., *J. Mater. Sci.*, 1990, **25**, 4175.
57. Berrod, G., Vidal, A., Papirer, E. and Donnet, J. B., *J. Appl. Polym. Sci.*, 1979, **23**, 2579.